

The Range of Alpha Particles in Air

Lennon Ó Náraigh, 01020021

Date of Submission: 5th April 2004

Abstract:

This experiment assumes that the notion of Range is applicable to alpha particles and sets out to calculate said range. In the course of the experiment, the dependence of the range on the geometry of the apparatus will be investigated.

In the experiment, it was found that $R_\alpha = 3.4 \pm 0.1 \text{ cm}$ for air at room temperature and atmospheric pressure. This compares well with the accepted value $R_\alpha = 3.4 \text{ cm}$ ¹. An estimate of the range of alpha particles in water was obtained from the Bragg-Kleeman rule, and was found to be $R_{\text{Water}} \sim [(0.16 \pm 0.01)\%] R_{\text{Air}}$.

¹ H.A. Bethe, *U.S. Atomic Energy Commission, Document BNL-T-7, 1949. Energy of alpha-particles: 4.88 MeV. These were the conditions of the experiment: Temperature of Air: 15°C; Pressure: 760 mm.*

Basic Theory and Equations:²

A realization of the foregoing theory is by 4.88MeV alpha particles (ions with $z = 2$) travelling through air. These are NR ($v \sim 10^7\text{ m/s}$). Alpha particles are highly ionizing and we expect these to interact strongly with matter. Thus, we expect the intensity of α -radiation to fall off steeply with source-detector distance and this will define the *range* – the distance at which the intensity becomes zero. This situation is contrasted with electrons, which do not interact so strongly with matter and thus do not exhibit the same strong range-intensity dependence.

The rate of a particle's (ion's) energy loss, per unit path length, as it passes through a medium, is known as the *stopping power*, S , of the medium. A quantum-mechanical derivation including relativistic effects was first carried out in 1930 by Bethe and Bloch, and their formula is quoted here:

$$S \equiv \frac{dE}{dx} = -(ze^2)^2 \frac{4\pi Z\rho N_A}{Amv^2} \left[\log\left(\frac{2mv^2}{I}\right) - \log(1 - \beta^2) - \beta^2 \right] \quad (1)$$

Where $v = \beta c$ is the ion velocity and ze is its electronic charge in e.s.u.'s, m the mass of the electron, A , Z , ρ are the atomic mass number, the atomic number and the density of the stopping material, respectively. I is the mean energy required to ionize a particle of the material and is about 86eV for air. As usual, terms in β can be dropped in the non-relativistic (NR) limit.

In a naïve treatment of equation³ (1), we might proceed in the following way:

$$\text{Write } \frac{dE}{dx} = -\frac{2C^2}{I} \frac{1}{\left(\frac{2mv^2}{I}\right)} \log\left(\frac{2mv^2}{I}\right) + o(\beta^4) \equiv -\frac{2C^2}{I} \frac{1}{\xi} \log\xi + o(\beta^4)$$

Where the terms in β^2 are self-cancelling.

$$\text{Then, } R = \int_0^R dx = \int_{E_0}^0 \frac{dx}{dE} dE = \frac{I}{2C^2} \int_0^{E_0} \frac{\xi}{\log\xi} dE, \text{ in the NR limit.}$$

Use $E = \frac{1}{2} M_\alpha v^2$ to change the variable of integration:

$$\xi = \frac{2mv^2}{I} = \frac{2m}{I} \left(\frac{1}{2} M_\alpha v^2 \right) \frac{2}{M_\alpha} = \frac{4m}{IM_\alpha} E$$

² John Lilley, *Nuclear Physics, Principles and Applications*, (Wiley, 2002), pp. 130 – 136.

³ <http://www.maths.tcd.ie/~olly/Lab.html> (Oliver Kelly)

$$\text{Hence, } R = \frac{I^2}{8C^2} \frac{M_\alpha}{m} \int_0^{\xi_0 = \frac{4m}{IM_\alpha} E_0} \frac{\xi}{\log \xi} d\xi = \frac{I^2}{8C^2} \frac{M_\alpha}{m} f(E_0) \quad (3)$$

However, this analysis is wrong. The integrand in (3) has a singularity at $E = \frac{IM_\alpha}{4m}$, i.e. when the travelling alpha particle has its energy reduced to $\sim 157 \text{ KeV}$. This reflects the fact that Bethe's formula is valid only in a *high-energy limit*. For, in the low-energy limit, the slow-moving alpha particles can themselves capture electrons, yet Bethe's formula does not consider this. The range, therefore, must always be calculated semi-empirically:

$$R = \int_0^R dx = \int_{E_0}^0 \frac{dE}{S} = \int_{E_0}^{T_2} \frac{dE}{S_B} + \int_{T_2}^{T_1} \frac{dE}{S_{\text{spline}}} + \int_{T_1}^0 \frac{dE}{S_E} \quad (4)$$

S_B is the stopping power according to Bethe's equation, valid in the range $[E_0, T_2]$. S_E is a function determined experimentally by fitting a curve to a stopping power versus energy dataset in the interval $[0, T_1]$, while "spline" is a cubic spline function fitted on the interval $[T_1, T_2]$ to ensure continuity between S_B and S_E . Typical values are $T_1 = 1.0 \text{ MeV}$ for helium ions, and $T_2 = 2.0 \text{ MeV}$ for helium ions.⁴

This semi-empirical approach gives a power law for R :⁵

$$R = \dots, E_0 \text{ in MeV} \quad (5)$$

(At STP).

Thus, for a 5 MeV alpha particle, $R = \dots$

⁴ <http://physics.nist.gov/PhysRefData/Star/Text/programs.html>

⁵ reference for power law

AIR (dry, near sea level)

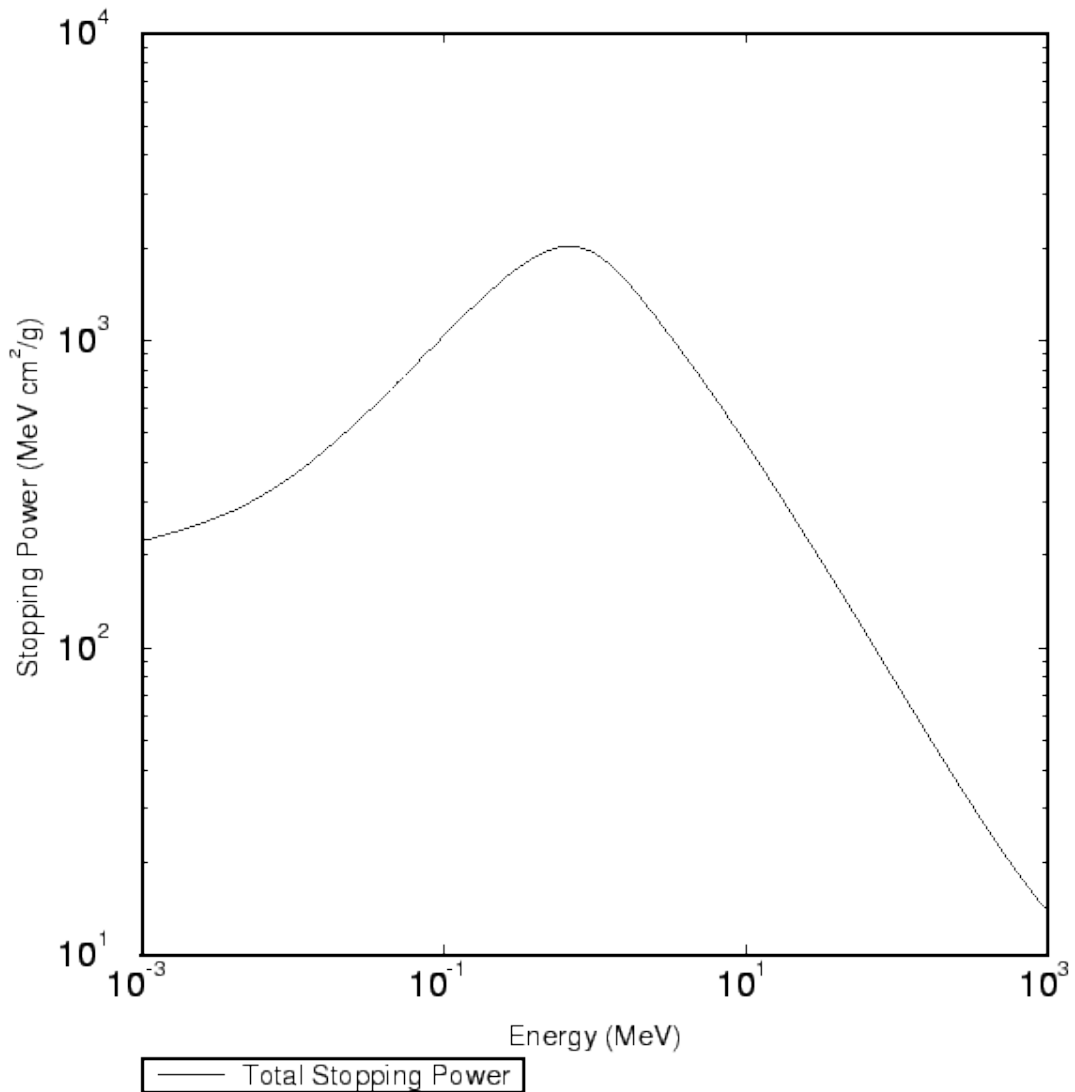


Figure 1. Stopping Power, S, as a function of initial energy, E₀. The decreasing tail represents the energy interval in which Bethe's formula is applicable. The low-energy limit is given by the empirical calculation, while the two regimes are joined continuously by a cubic spline. (From http://physics.nist.gov/cgi-bin/Star/ap_table.pl).

This compares with the standard, experimental value for a 5 MeV alpha particle at STP got from the following calculation:

$$R = 4.368 \times 10^{-3} \text{ g/cm}^2 \text{ } ^6$$

$$\Rightarrow R = (4.368 \times 10^{-3} \text{ g/cm}^2) \times (\rho_{\text{air}} = 1.3 \times 10^{-3} \text{ g/cm}^3) = 3.49 \text{ cm}$$

⁶ http://physics.nist.gov/cgi-bin/Star/ap_table.pl

For any material, we see from equation (1), or from intuitive considerations, that $\left| \frac{dE}{dx} \right| \propto \rho$. Dividing equation (1) by ρ and considering one kind of projectile only, we get

$$\frac{1}{\rho} \frac{dE}{dx} \propto \frac{Z}{A} \log \left(\frac{2mv^2}{I(Z_{Material})} \right) \quad (6)$$

Here, the factors $\frac{Z}{A}$ and the logarithm vary slowly.

The Bragg-Kleeman rule estimates the density-dependence of the range through the following empirical relationship:

$$\frac{R_1}{R_2} \approx \frac{\rho_2 \sqrt{A_1}}{\rho_1 \sqrt{A_2}} \quad (7)$$

Where the indices 1 and 2 refer to the first and second media, respectively.

As well as the I, E and ρ dependence of the stopping process outlined, there is a statistical element involved. For, there is a variation in the energy transfer per collision and in the amount of ionization produced by a given energy loss distance travelled. Thus, there is a spread in the observed range of monoenergetic particles, called *straggling*. However, this is not significant for heavy charged particles like alpha particles – for 5MeV alpha particles, the standard deviation of the range distribution is about 1%⁷

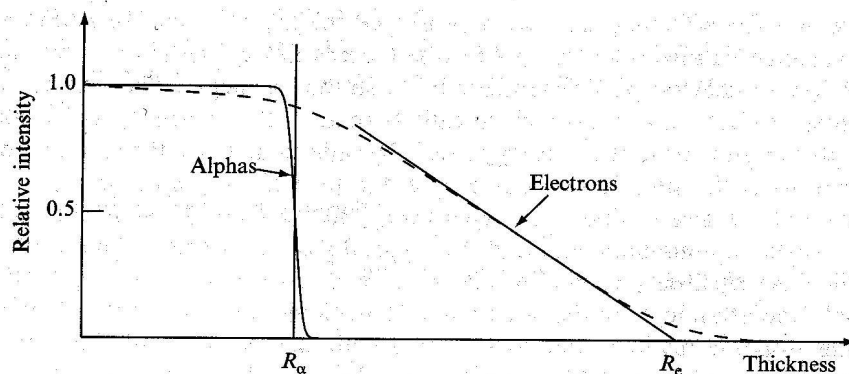


Figure 2. Relative intensity as a function of distance travelled for alpha particles and electrons. After Lilly, p. 136.

This suggests that we can model the relative intensity as a function of distance as a Fermi function:

$$y(x; \lambda_1, \lambda_2, \lambda_3) = \frac{\lambda_1}{e^{(x-\lambda_2)/\lambda_3} + 1} \quad (8)$$

Detection of Alpha Particles:

⁷ Lilly, p 134.

In this experiment, we use a photomultiplier tube as a counter, whose entrance window is coated with ZnS scintillator powder. The pulses from the photomultiplier pass via an amplifier to a pulse counter.

There are two types of scintillator powders. One is *organic*, and such a material is not a semiconductor. Such a material has two widely spaced electronic energy levels \mathcal{E}_0 and \mathcal{E}_1 , say, and around these levels there are many vibrational levels $\mathcal{V}_{01}^0, \mathcal{V}_{02}^0, \dots; \mathcal{V}_{11}^0, \mathcal{V}_{12}^0, \dots$. An incident particle interacts with the scintillator powder and raises the molecules of the material from a 0 level to a 1 level. The material then deexcites and emits a scintillation photon in the visible range. Because of the level scheme, very few scintillation photons can raise the material itself to an excited level. Thus, the scintillator powder is transparent to its own radiation.

The other type of scintillator powder is *inorganic* and many of these are alkali halides, such as NaI. Such materials crystallize and have semiconductor properties. Thus, there is a filled band (a group of adjacent electronic states in k -space) and an unfilled band, separated by a bandgap. Incident, energetic particles can cause the excitation of a valence electron (electron in the filled band) into the conduction band (the empty or part-filled band). On deexcitation, the electron emits a scintillation photon. However, in general this photon is in turn, capable of exciting a valence electron, and so such a material is not transparent to its own radiation. It is only through the addition of a small amount of impurity to the crystal that the transparency can occur. For, the impurity provides the electron with allowed states in the bandgap, and deexcitation from these states will not lead to a photon capable of reexciting electrons.

Figure 3. Energy level schemes for organic and inorganic scintillator powders.

Method and Results:

- (i) To measure the count rate C as a function of the source-detector distance, d .

The following graph was obtained:

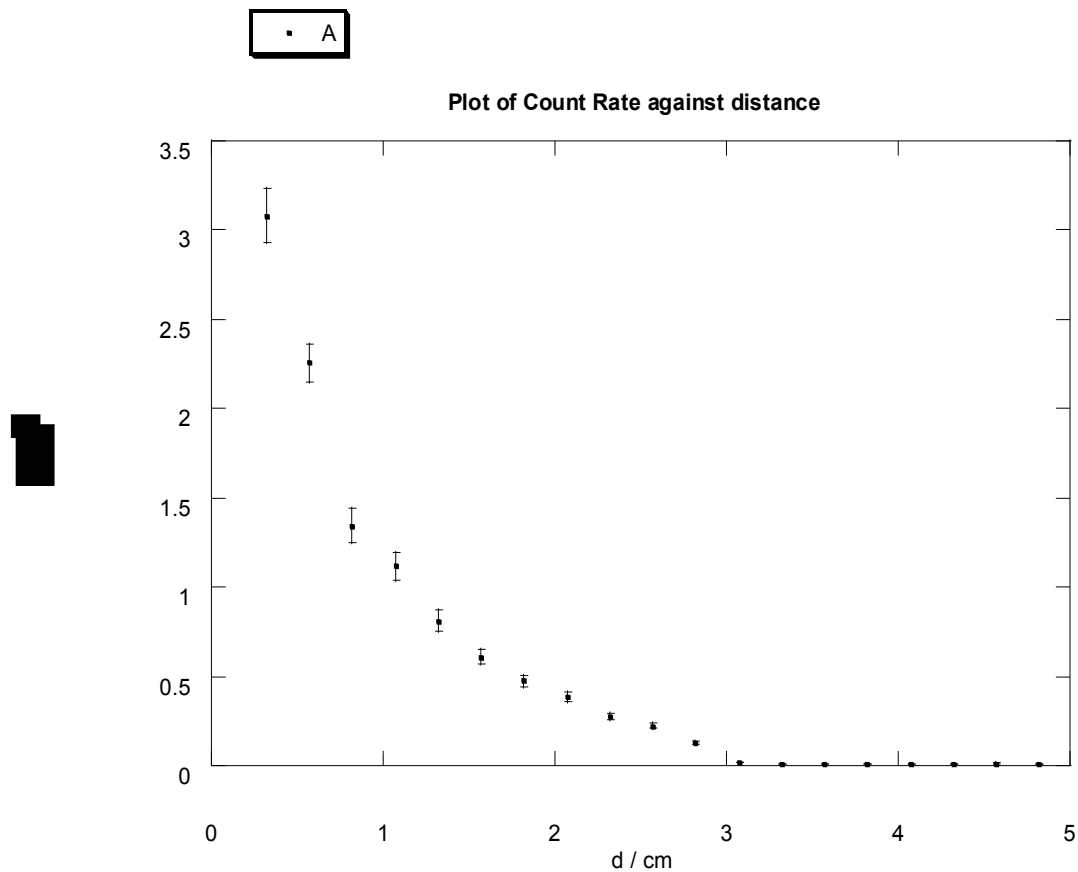


Figure 4. Plot of Count rate, C , against the source-detector distance, d .

This curve is not found to decrease to zero as sharply as the Fermi function. This is because the probability of detection by the counter is proportional to the area of the detector (a constant), and the source-detector distance only. Thus, in later sections, we study the quantity $\frac{dC}{d\Omega} = f(\theta, \phi, d)$, while here we examine $C(d) = \int_{4\pi} f(\theta, \phi, d)$.

(ii) To measure the count rate per unit solid angle ($\frac{C}{\Omega}$) against the source-detector distance d , assuming that the source is point-like and the detector can be modelled as a spherical cap.

Now the spherical cap is the curved surface area of a segment of sphere, although this is approximated by $A_{cap} \approx \pi (R_{aperture} = 0.533cm)^2$, where $R_{aperture}$ is the radius of the detector aperture. Thus, we approximate Ω by $\frac{A_{cap}}{d^2}$

The exact result is obtained from integration and the derivation is in appendix 1:

$$\Omega(x, R) = 4 \arctan\left(\frac{R}{x}\right) \frac{R}{\sqrt{x^2 + R^2}} \quad (9)$$

This dependence is exhibited in the following graph:

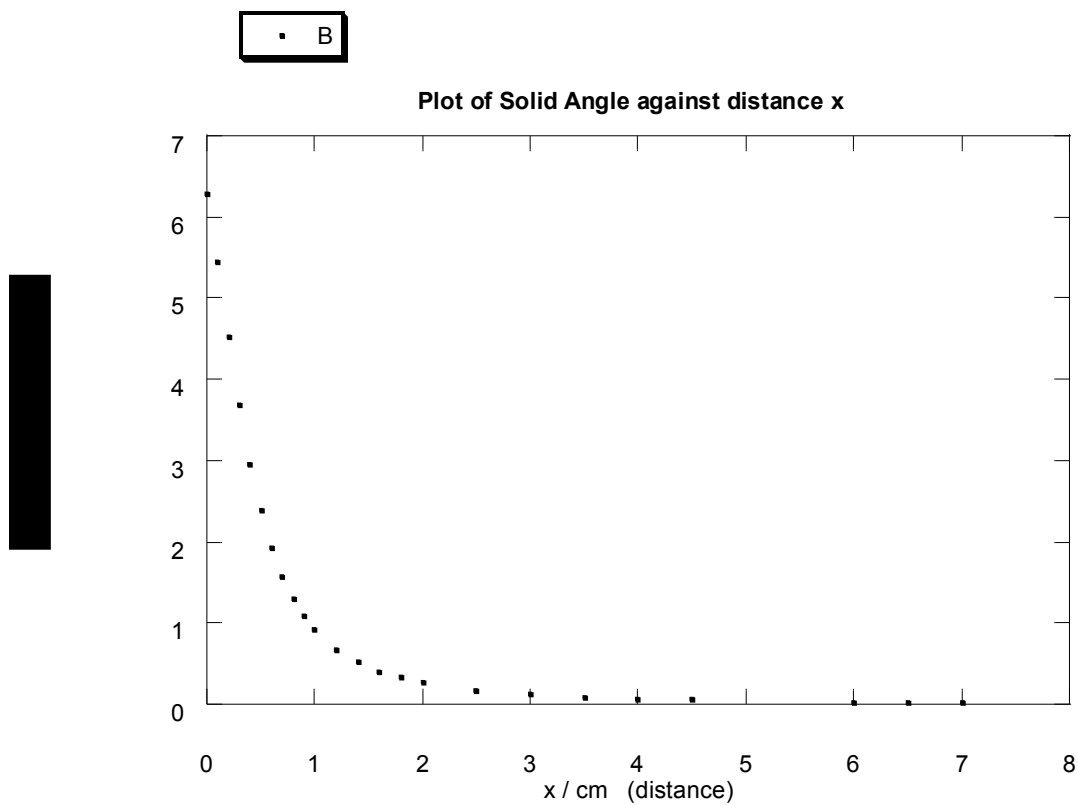


Figure 5. Plot of Solid angle against the distance x for a point-like source and a spherical cap. (Geometry illustrated in appendix A).

The following plot was obtained for $\frac{C}{\Omega}$ versus d .

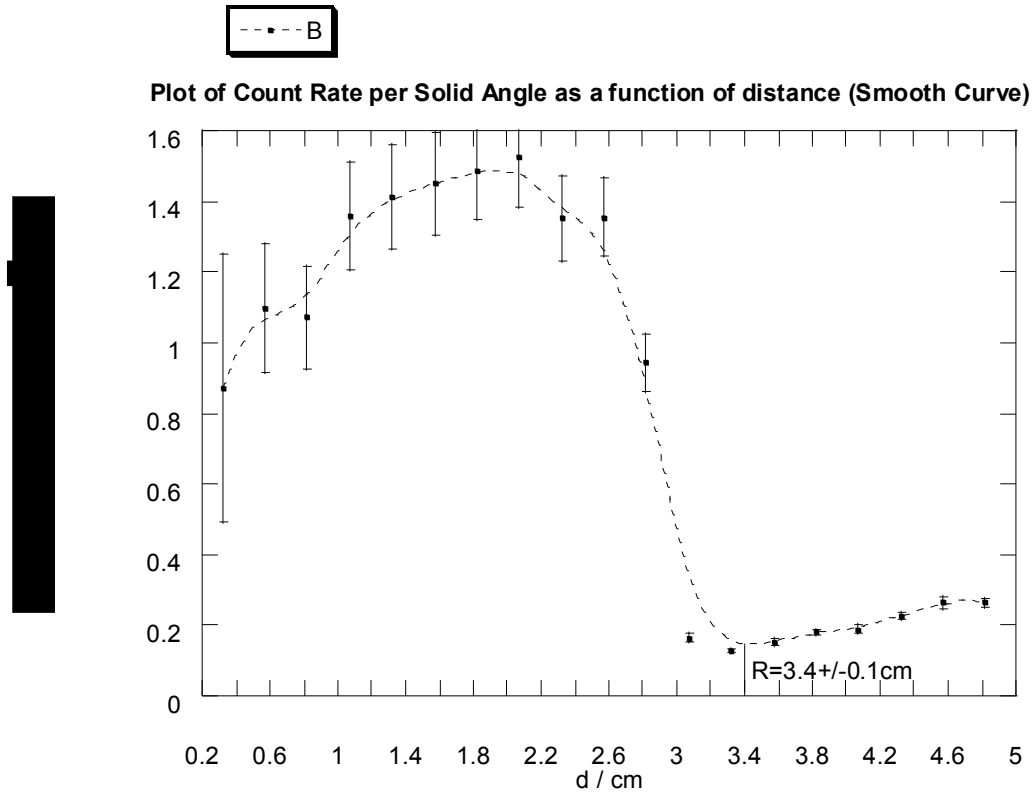


Figure 6. Plot of count rate per solid angle as a function of source-detector distance, d for the assumption of point-like source. A smooth curve has been fitted.

This gives a value for the range of $R_{\alpha} = 3.4 \pm 0.1 \text{ cm}$. This compares with Bethe's value of $R_{\alpha} = 3.4 \text{ cm}$

(iii) Examining the behaviour of $\frac{C}{\Omega}$ as a function of d assuming that the source is finite in extent:

The geometry of this situation is considered in appendix 2. We get the following calibration curve for Ω as a function of R / d , and we estimate the functional form as a power series, truncating after five terms.

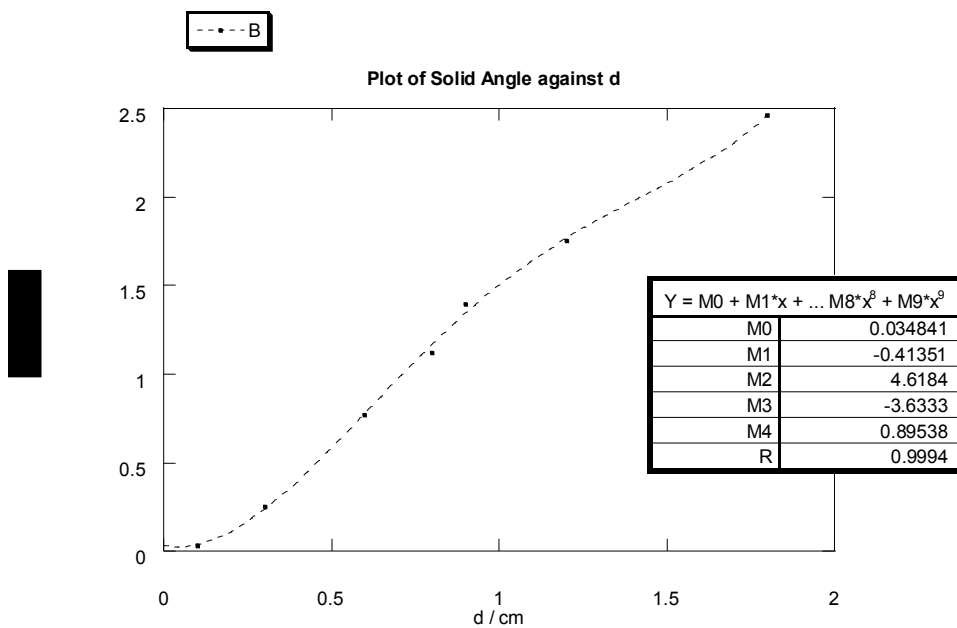


Figure 7. Plot of Solid angle against source-detector distance d . (Geometry indicated in Appendix B).

The following plot of $\frac{C}{\Omega}$ as a function of source-detector distance d is obtained:

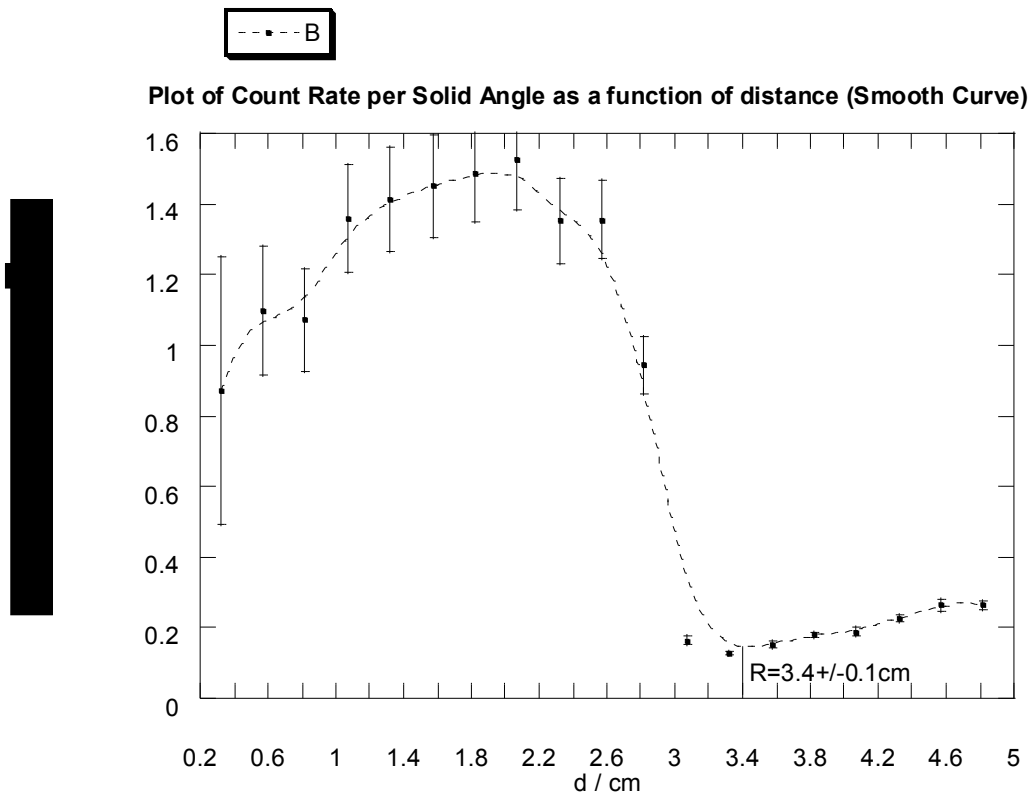


Figure 8. Plot of count rate per solid angle as a function of source-detector distance, d for the assumption of non-point-like source geometry. A smooth curve has been fitted.

Again, we find that $R_{\alpha} = 3.4 \pm 0.1 \text{ cm}$.

Further Questions:

We could estimate the range of alpha particles in water using the Bragg-Kleeman rule, mentioned in the Theory section:

$$\frac{R_1}{R_2} \approx \frac{\rho_2 \sqrt{A_1}}{\rho_1 \sqrt{A_2}} \quad (7)$$

Where A is the mass number of the medium in which the ions travel.

Taking $R_{air} = 3.0 \pm 0.5 \text{ cm}$ from the first experiment, $A_{air} \approx A_{Nitrogen} = 7$, $A_{Water} \approx 10$ (defining an “effective” mass number for water as $8 + 1 + 1$) and $\rho_{air} = 1.299 \text{ kg / m}^3$ ⁸, we get

$$R_{Water} \sim (0.16\%)R_{Air}$$

It is more difficult to arrange a similar experiment for electrons (say). This is because electrons interact less with matter and are more likely to pass through a material unaffected. Thus, we would expect a more gradual fall off in electron intensity as a function of source-detector distance, making the notion of range difficult to apply.

The anomaly in figures 6 and 8:

In both figures 6 and 8 we see that the count rate per unit solid angle starts to *increase* once the range has been reached. This may be due to gamma emission by excited Po nuclei. For, an alpha particle may tunnel out of the nucleus at a lower energy than the expected 4.88 MeV. The unstable nucleus must then decay to the ground state by the emission of a gamma ray. It is possible that this gamma radiation explains the non-zero intensity observed once the travelling alpha particles have exceeded their range.

Uncertainty in Measurements:

In the second experiment, the sources of error are the following:

- The usual measurement errors (distance d , count rate C : $\delta N = \sqrt{N}$).
- The error incurred by reading the range from figure...

In the third experiment, the sources of error could be found among the following:

⁸ <http://wright.nasa.gov/airplane/airprop.html> At STP

- The error incurred in fitting a polynomial to the datapoints of $\Omega(d)$. This manifests itself in the large error bars in figure... These were derived from the following considerations:

$$\Omega(d) = \sum_{n=0}^N \alpha_n \left(\frac{R}{d}\right)^n \Rightarrow \delta\Omega(d) = \sum_{n=0}^N \alpha_n \left(\frac{R}{d}\right)^n \left[\frac{\delta\alpha_n}{\alpha_n} + \frac{\delta d}{d} \right]$$

and by assuming that $\frac{\delta\alpha_n}{\alpha_n} \sim 5\%$

- The sparsity of data points in the critical region where the intensity falls to zero (or to background) rapidly.

Conclusions:

In this experiment it was found that the range of alpha particles in air is $R_\alpha = 3.4 \pm 0.1 \text{ cm}$, which agrees with Bethe's result. This measurement was accomplished by first of all assuming a point-like source and subsequently, by correcting for this assumption. In both cases, the result was the same.

The Bragg-Kleeman rule was used to estimate the range of alpha particles in water, and this was found to be $54 \pm 3 \mu\text{m}$. This is to be compared with $38 \mu\text{m}$ for 5 MeV alpha particles in liquid form.⁹ This suggests either that the Bragg-Kleeman rule is capable only of predicting relative ranges only to orders of magnitude, or that we find a more sophisticated way of defining "effective mass numbers" for molecules such as water. This question should certainly be investigated.

⁹ http://physics.nist.gov/cgi-bin/Star/ap_table.pl

Appendix 1:

The derivation of the equation $\Omega(x, R) = 4 \arctan\left(\frac{R}{x}\right) \frac{R}{\sqrt{x^2 + R^2}}$ (9).

Assume a point-like source radiating into a spherical cap and viewed in the coordinate system shown below:

$$dA = d^2 d\Omega \Rightarrow A = d^2 \int d\Omega$$

$$\int d\Omega = 2 \int_0^\phi d\phi \int_\theta^{\theta+2\phi} \sin\theta d\theta = -2\phi \cos\theta \Big|_\theta^{\theta+2\phi}$$

$$\cos(\theta + 2\phi) - \cos\theta = \cos\theta \cos 2\phi - \sin\theta \sin 2\phi - \cos\theta$$

$$\dots = \frac{R}{\sqrt{x^2 + R^2}} \left[\left(\frac{x}{\sqrt{x^2 + R^2}} \right)^2 - \left(\frac{R}{\sqrt{x^2 + R^2}} \right)^2 \right] - 2 \frac{x}{\sqrt{\dots}} \frac{x}{\sqrt{\dots}} \frac{R}{\sqrt{\dots}} - \frac{R}{\sqrt{\dots}}$$

$$\dots = \frac{-2R}{\sqrt{x^2 + R^2}}$$

$$\int d\Omega = 4\phi \frac{R}{\sqrt{x^2 + R^2}} = 4 \arctan\left(\frac{R}{x}\right) \frac{R}{\sqrt{x^2 + R^2}} \quad (9)$$

Appendix 2:

The source of finite extent: It is not legitimate to model the apparatus as a spherical cap-like detector and a point-like source. Indeed, the source is finite in extent and this becomes important for small source-detector distances.

In the case of a circular disc of radius S facing another smaller circular disc of radius R (figure...), the solid angle at one disc subtended by the other is

$$\Omega\left(\frac{R}{d}, \frac{S}{d}\right) = \frac{\int_0^S \Omega(d, R, x) x dx}{\int_0^S x dx}$$

(10)

We tabulate $\Omega\left(\frac{R}{d}, \frac{S}{d}\right)$ for the special case where $R = S$ and find all values of $\Omega(d)$ by means of a graph (figure 7). With this assumption, the source and detector have the same surface area.